Optical Wavelet Transform of Fractal Aggregates

E. Freysz,[2] B. Pouligny,[1] F. Argoul,[1] and A. Arneodo[1]
[1]*Centre de Recherche Paul Pascal, Domaine Universitaire, 33405 Talence CEDEX, France*
[2]*Centre de Physique Moléculaire Optique et Hertzienne, Université de Bordeaux I, 351, Avenue de la Libération, 33405 Talence CEDEX, France*
(Received 22 May 1989)

Wavelet transformations (WT's) of two-dimensional fractal aggregates are carried out using coherent optical spatial-frequency filtering. The ability of optical WT's to reveal the construction rules of fractals and to resolve local scaling properties through the determination of local pointwise dimensions is demonstrated. This fast method paves the way to time-resolved studies of dynamical phenomena.

PACS numbers: 42.30.−d, 07.60.−j, 61.50.Cj, 64.60.Ak

In the past decade, much effort has been devoted to the characterization of fractal aggregates arising in a variety of theoretical and experimental situations.[1,2] In early studies,[2] most of the descriptions have focused on a few particular meaningful dimensions:[3] the fractal or *capacity* dimension D_0, the *information* dimension D_1, and the (two-point) *correlation* dimension D_2. These dimensions can be measured using numerical methods.[4] On the other hand, optics and, more generally, radiation diffraction are known to be a cheap and fast way of calculating spatial Fourier spectra and have proved powerful in experimental studies of various fractals.[5] However, the estimate of D_0, D_1, or D_2 provides only limited information on the structural complexity of fractals. Recently, attention has been paid to the computation of the whole spectrum of generalized fractal dimensions[3] D_q. These dimensions are closely related to the $f(\alpha)$ spectrum[6] of singularities of strength α. According to these mathematical concepts, fractals can be classified into two families: (i) *uniform* (globally self-similar) fractals for which all the D_q's coincide, i.e., their $f(\alpha)$ spectrum is concentrated on a single point $\alpha=D_0$; and (ii) *multifractals*,[6] which are usually characterized by a monotonic decreasing dependence of D_q vs q, and in which case, α is no longer unique and $f(\alpha)$ turns out to be a single-humped function of maximum D_0.

Measurements of the D_q's and $f(\alpha)$ curves only provide a global statistical information about the scaling properties of fractals. In fact, these quantities do not fully characterize the local self-similarity of fractals since they do not keep track of the spatial location of the singularities. A known method which comes close to satisfying this requirement is the *wavelet transform*[7] (WT). This mathematical technique has been introduced in a recent analysis[8] of seismic data and acoustic signals to overcome the inability of the Fourier analysis to locate the underlying frequencies. Since then, this "time-frequency" analysis has been applied in many different fields.[7] In particular, the WT has been emphasized to be a natural tool for investigating the self-similar properties of fractal objects at different length scales.[9-11] Very recently, this multiscale analysis has been further extended to multidimensional signals[11,12] and its efficiency has been tested[13] on fractals such as snowflakes and diffusion-limited aggregates (DLA). However, the implementation of the two-dimensional WT on a computer can be time consuming when a high resolution is required. An alternative method consists of using a coherent optical trick to perform the WT in real time. In this Letter, we describe a setup which optically performs the WT and we demonstrate the capability of this technique to characterize the local scaling properties of fractals.

The WT of a one-dimensional signal consists in decomposing the signal into elementary contributions, the so-called *wavelets*, which are constructed from one single function g by means of dilations and translations.[7,8] The generalization to higher dimensions involves rotations as well.[12] Hence, let us consider a fractal represented by a real function f over $\mathcal{R}^n$, and let $d\mu(\mathbf{x})=f(\mathbf{x})d^nx$ be the measure with density $f(\mathbf{x})$ (in practice, a mass density); let g be a regular complex-valued function over $\mathcal{R}^n$ that is localized around the origin and some of whose moments are zero [g should be at least of zero mean, $\int d^nx\, g(\mathbf{x})=0$, for the wavelet to be admissible]. The WT of f with respect to the wavelet g is defined as

$$T_g(a,r,\mathbf{b})=a^{-n}\int g^*(a^{-1}r^{-1}(\mathbf{x}-\mathbf{b}))f(\mathbf{x})d^nx \quad (1a)$$

$$=\int e^{i\mathbf{q}\cdot\mathbf{b}}\hat{g}^*(ar^{-1}\mathbf{q})\hat{f}(\mathbf{q})d^nq\,, \quad (1b)$$

where the asterisk denotes the complex conjugate and the caret the Fourier transform; a, r, and $\mathbf{b}$ are the dilation parameter ($a>0$), the n-dimensional rotation operator [$R^rg(\mathbf{x})=g(r^{-1}\mathbf{x})$], and the displacement vector, respectively. Whenever g is admissible, no information about f is lost since this transformation is likely to be invertible[12] for a large class of functions f. T_g is generally a complex-valued function. This transformation can be seen as a "mathematical microscope"[9-11,13] whose position and magnification are $\mathbf{b}$ and $1/a$, respectively,

and whose optics is given by the choice of the analyzing wavelet g. Of course, this microscope is isotropic only if g is radially symmetric. A very popular analyzing wavelet in $\mathcal{R}^2$ is the so-called radial Mexican hat,[11-13] $g(\mathbf{x})=(2-\mathbf{x}^2)e^{-\mathbf{x}^2/2}$. In the following, we will restrict the discussion to radially symmetric WT's (in fact, only basically isotropic procedures have been used in most calculations of local dimensions[4]). The possibility of using nonradial wavelets, however, looks very attractive to study fractals which do not scale isotropically.

A typical property of fractals is that they are asymptotically self-similar at small length scales.[1] Local self-similarity means that the fractal measure μ scales around the point $\mathbf{x}_0$ as

$$\mu(\mathcal{B}(\mathbf{x}_0,\lambda\epsilon))\sim\lambda^{\alpha(\mathbf{x}_0)}\mu(\mathcal{B}(\mathbf{x}_0,\epsilon)), \quad (2)$$

where $\mathcal{B}(\mathbf{x}_0,\epsilon)$ is an ϵ-ball centered at $\mathbf{x}_0$. The wavelet transform of μ in turn scales as[10,11,13]

$$T_g(\lambda a,\mathbf{x}_0)\sim\lambda^{\alpha(\mathbf{x}_0)-n}T_g(a,\mathbf{x}_0). \quad (3)$$

Thus, from the power-law behavior of T_g one can extract the strength $\alpha(\mathbf{x}_0)$ of the singularities located at $\mathbf{x}_0$.

In terms of computer time, high-resolution two-dimensional numerical WT's are expensive. Equation (1b) shows that the WT just amounts to filtering the Fourier spectrum of f by $\hat{g}(a\mathbf{q})$. Performing the WT optically then just needs a proper coherent optical filtering of the aggregate, at task which can be easily achieved in a classical double Fraunhofer diffraction geometry. Figure 1 shows our optical wavelet transform (OWT) setup. The beam of a linearly polarized He-Ne laser (wavelength $\lambda=632.8$ nm, power ~ 10 mW) is focused by a microscope lens M_1 onto a small pinhole P (12.5 μm in diameter). P is located in the front focal plane of the lens L_1 ($f_1=1$ m, diameter $=5$ cm). A large-diameter nearly parallel and uniform beam comes out of L_1. The sample to be wavelet transformed is in the form of a 35-mm slide. The ones used in this preliminary study were built starting from computer-generated fractals, which were first drawn with a laser printer and photographed using a high-resolution 35-mm black and white film. The slide is located after L_1, in the front focal plane of a second converging lens L_2, of same characteristics as L_1. The electromagnetic field distribution at any point $\mathbf{u}$ in the rear focal plane of L_2 is proportional to $\hat{f}(\mathbf{q}=(2\pi/\lambda f_1)\mathbf{u})$. The filtering [Eq. (1b)] is carried out in this plane. Filters used up to now are just transparent rings, which select spatial frequencies $\mathbf{q}$ such that $q_1\le aq\le q_2$. q_1 and q_2 are constants, which can be chosen arbitrarily [see Fig. 1(a)]. Notice that such a filtering is a binary approximation of the Fourier transform of the radial Mexican hat.[11,13] The filters were built using the same photographic procedure as for the samples. The parameter a defines the scale of the OWT. The filter is located in the front focal plane of a third lens L_3 ($f_3=0.3$ m), which images the filtered sample, i.e., its wavelet transform, in its rear focal plane. Performing the whole wavelet transform [Eq. (1)] just amounts to repeating the same operation with different values of a, in practice with a stack of up- and down-scaled versions of one particular filter. The maximum value $a_{\max}$ of a is limited by the size of the focal spot given by L_2. $a_{\min}$ is limited by the size of the lattice on which the fractals are generated. The filtered image is sent to a charge-coupled device (CCD) camera and to a Pericolor 2001 image processor. Since the camera is a quadratic detector, the setup in fact gives $|T_g(a,\mathbf{b})|^2$. The intensities of the OWT's are kept within the range of linearity of the camera by adjusting the power of the He-Ne beam.

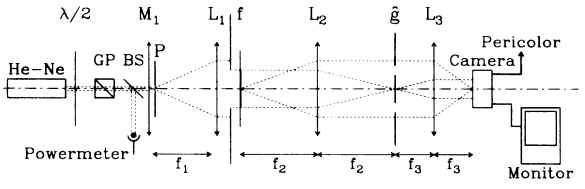

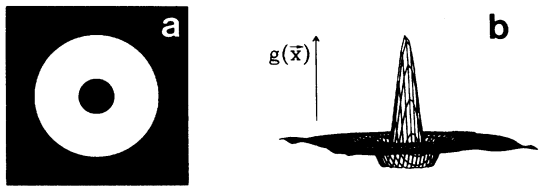

FIG. 1. Experimental setup. The intensity of the He-Ne laser is tuned by means of a half-wave plate associated with a Glan-prism (GP) polarizer, and monitored by means of a powermeter. f: fractal sample. (a) The Fourier transform $\hat{g}(\mathbf{q})$ of the analyzing wavelet; (b) the corresponding analyzing wavelet $g(\mathbf{x})$.

If the mass density of the fractal scales around the point x_0 with the local exponent $\alpha(\mathbf{x}_0)$ [Eq. (2)], then the intensity recorded at this point on the CCD camera will behave like

$$I(\lambda a,\mathbf{x}_0)=|T_g(\lambda a,\mathbf{x}_0)|^2\sim\lambda^{2[\alpha(\mathbf{x}_0)-2]}|T_g(a,\mathbf{x}_0)|^2, \quad (4)$$

i.e., with a scaling exponent $\beta(\mathbf{x}_0)=2[\alpha(\mathbf{x}_0)-2]$.

In Figs. 2(b)-2(d) we present an overview of the OWT of the snowflake fractal[13] shown in Fig. 2(a). The OWT is shown for decreasing values of the scale parameter a. This OWT "zooming" provides conspicuous information about the construction rule of the snowflake. At large scale, one observes a single object of length size a^*. In the next step, this object is divided into nine identical pieces, each of which is a reduced version of the original object with length scale $a^*/3$ [Fig. 2(b)]; four among the nine pieces are removed, while the central piece with the four pieces at each corner are retained.[14] Then the same procedure is repeated in the next step for each of the five remaining pieces [Fig. 2(c)]. The

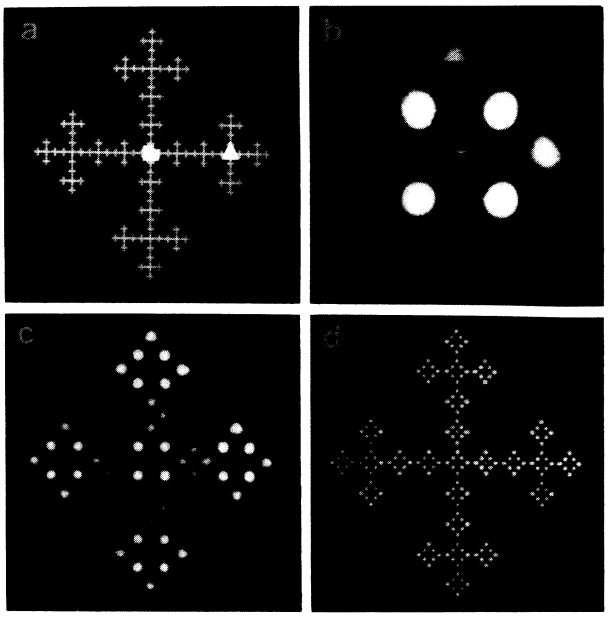

FIG. 2. (a) Snowflake fractal, and its OWT's at different scales: (b) $a=a^*/3$, (c) $a^*/3^2$, and (d) $a^*/3^3$. Pictures show rescaled intensities $S(a,\mathbf{b})=a^{-\beta}I(a,\mathbf{b})$; $\beta=2(\alpha_{SF}-2)$, $\alpha_{SF}=\log 5/\log 3$.

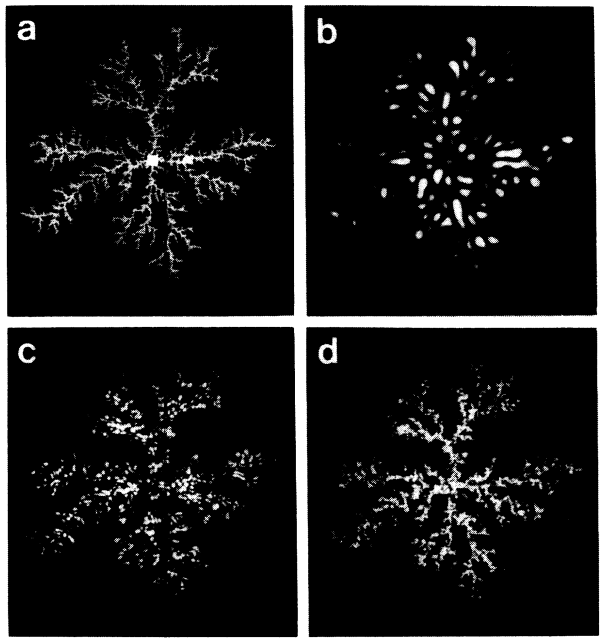

FIG. 3. (a) DLA fractal, and its OWT's at different scales: (b) $a=a^*$, (c) $a^*/3^{9/10}$, and (d) $a^*/3^{9/5}$. The intensity of the laser was tuned so as to keep the intensity maxima nearly independent of the filter size.

snowflake [Fig. 2(a)] is indeed obtained by applying the same rule subsequently [Fig. 2(d)] *ad infinitum*.[13] Besides its edge-detection ability, the OWT provides clear evidence for the global self-similarity of snowflake fractals; at each point **b** of the aggregate, the OWT displays a power-law behavior with an exponent $\beta=2(\alpha_{SF}-2)$ independent of **b**. The values of this exponent at two different points of the aggregate were determined from the graph shown in Fig. 4, where the intensity I is plotted versus a in a log-log scale representation. Disregarding finite-size effects and despite intrinsic oscillations[10,11,13] in the log-log procedure due to the lacunarity of the snowflake, the OWT provides an estimate of the exponent α_{SF} in good agreement with the theoretical prediction $\alpha_{SF}=\log 5/\log 3$, and previous numerical wavelet transform analysis.[13]

Figure 3 shows the OWT of a DLA cluster of mass $M=13000$ particles through different panels corresponding to increasing values of the magnification a^{-1}. This aggregate [Fig. 3(a)] was computed with the random-walker model of Witten and Sander.[15] As expected from our previous OWT analysis of snowflake fractals, this method provides insight into thinner and thinner internal details in the shape of DLA patterns. At large scale [Figs. 3(b) and 3(c)], DLA clusters look very much like viscous fingers[2] observed in Hele-Shaw experiments. When looking at smaller scales, the main fingers split into fingers of smaller width [Fig. 3(c)] and successive generations of fingers show up [Fig. 3(d)], leading to the arborescent structure of DLA clusters [Fig. 3(a)]. But what is remarkable in Fig. 3 is that successive generations appear at the same rate when the magnification is increased (in logarithmic scale). This observation strongly suggests that DLA clusters are very likely to display global invariance. In Fig. 4, the intensity I of the OWT is plotted versus a in a log-log representation. To the previously mentioned experimental difficulties encountered at small and large scales, additional theoretical difficulties (intrinsic aperiodic oscillations in the log-log procedure) inherent to these chaotic fractals[13] make the measurement of the local scaling index $\beta=2[\alpha_{DLA}(\mathbf{b})-2]$ more demanding.[16] The data collected for two points of the DLA cluster [Fig. 3(a)], together with a mean value of the intensity of the OWT over the whole aggregate, confirm the conclusion of previous numerical studies[13,17] and bring direct evidence for the self-similarity of DLA clusters with a unique scaling exponent $\alpha_{DLA}\sim 1.60$.

To summarize, we have presented an experimental arrangement which performs the OWT of two-dimensional objects. This optical transform was tested on globally self-similar fractal aggregates, and a remarkable agreement was found with the results of previous numerical studies.[13] Further analysis of multifractal aggregates are currently in progress and some opening does exist in three dimensions. The ability of the OWT to operate in real time provides a very efficient method for characterizing not only static situations but also dynamical phenomena. The application of the OWT to a variety of experimental situations, e.g., percolation, colloidal aggre-

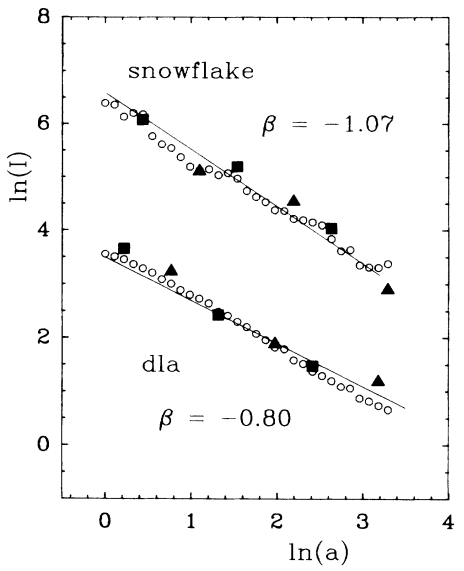

FIG. 4. Intensities of the OWT's of the snowflake and DLA clusters vs the filter size, in log-log representation. ■ and ▲ : data collected when pointing the OWT at two different points of the aggregate [see Figs. 2(a) and 3(a)]; ○: average of the intensity I over the whole aggregate. Different arbitrary units have been used for the different sets of intensities since only slopes are relevant. The solid lines correspond to the theoretical prediction $\beta=2(\alpha_{SF}-2)=-1.07$ for the snowflake ($\alpha_{SF}=\log 5/\log 3$), and to a previous numerical estimate (Ref. 13) $\beta=2(\alpha_{DLA}-2)=-0.8$ for the DLA cluster ($\alpha_{DLA}\simeq 1.60$).

gation, growth phenomena, fracture patterns, nucleation, two-dimensional melting, and turbulent flow,[18] looks very promising.

We would like to thank C. Froehly for very interesting suggestions in the design of the optical filtering procedure, and J. F. Muzy and G. Grasseau for helpful discussions and numerical assistance.

[1]B. B. Mandelbrot, *The Fractal Geometry of Nature* (Freeman, San Francisco, 1982).

[2]*On Growth and Form: Fractal and Nonfractal Patterns in Physics,* edited by H. E. Stanley and N. Ostrowsky (Martinus Nijhoff, Dordrecht, 1986); *Fractals in Physics,* edited by L. Pietroniero and E. Tosatti (North-Holland, Amsterdam, 1986); *Statphys 16,* edited by H. E. Stanley (North-Holland, Amsterdam, 1986); *Random Fluctuations and Pattern Growth: Experiments and Models,* edited by H. E. Stanley and N. Ostrowsky (Kluwer Academic, Dordrecht, 1988).

[3]P. Grassberger and I. Procaccia, Physica (Amsterdam) **13D**, 34 (1984).

[4]*Dimensions and Entropies in Chaotic Systems,* edited by G. Mayer-Kress (Springer-Verlag, Berlin, 1986).

[5]C. Allain and M. Cloitre, Phys. Rev. B **33**, 3566 (1986).

[6]R. Benzi, G. Paladin, G. Parisi, and A. J. Vulpiani, J. Phys. A **17**, 3521 (1984); T. C. Halsey, M. H. Jensen, L. P. Kadanoff, I. Procaccia, and B. I. Shraiman, Phys. Rev. A **33**, 1141 (1986); P. Collet, J. Lebowitz, and A. Porzio, J. Stat. Phys. **47**, 609 (1987).

[7]*Wavelets,* edited by J. M. Combes, A. Grossmann, and P. Tchamitchian (Springer-Verlag, Berlin, 1989).

[8]P. Goupillaud, A. Grossmann, and J. Morlet, Geoexploration **23**, 85 (1984); A. Grossmann and J. Morlet, in *Mathematics and Physics, Lectures on Recent Results,* edited by L. Streit (World Scientific, Singapore, 1985); R. Kronland-Martinet, J. Morlet, and A. Grossmann, Int. J. Pattern Recognit. Artif. Intelligence **1**, 273 (1987).

[9]M. Holschneider, J. Stat. Phys. **50**, 963 (1988).

[10]A. Arneodo, G. Grasseau, and M. Holschneider, Phys. Rev. Lett. **61**, 2281 (1988); in Ref. 7, p. 182.

[11]A. Arneodo, F. Argoul, J. Elezgaray, and G. Grasseau, in *Nonlinear Dynamics,* edited by G. Turchetti (World Scientific, Singapore, 1988), p. 130.

[12]R. Murenzi, in Ref. 7, p. 239.

[13]F. Argoul, A. Arneodo, J. Elezgaray, G. Grasseau, and R. Murenzi, Phys. Lett. **135A**, 327 (1989); Phys. Rev. A (to be published).

[14]Let us note that, at a given step in the construction process, the negative parts of the WT that correspond to the removed pieces contribute constructively to the recorded intensity $[I\sim|T_g(a,\mathbf{b})|^2]$. But these negative parts can be easily distinguished from the positive parts which delimit the retained pieces because they completely vanish at the next step.

[15]T. Witten and L. M. Sander, Phys. Rev. Lett. **47**, 1400 (1981); Phys. Rev. B **27**, 5686 (1983).

[16]The analyzing wavelet used in this preliminary study displays an oscillatory decreasing tail at large $|\mathbf{x}|$. When studying fractal aggregates of finite size, this oscillatory tail produces oscillations in $T_g(a,\mathbf{x})$ vs a log-log plots which superpose on the intrinsic oscillations due to the lacunarity of the aggregates. We have checked that with our experimental setup, the amplitude of these oscillations does not seriously affect the estimate of the local scaling exponent for $\alpha(\mathbf{b})\leq 2$.

[17]F. Argoul, A. Arneodo, G. Grassaeu, and H. L. Swinney, Phys. Rev. Lett. **61**, 2558 (1988).

[18]F. Argoul, A. Arneodo, G. Grasseau, Y. Gagne, E. Hopfinger, and U. Frisch, Nature (London) **338**, 51 (1989).

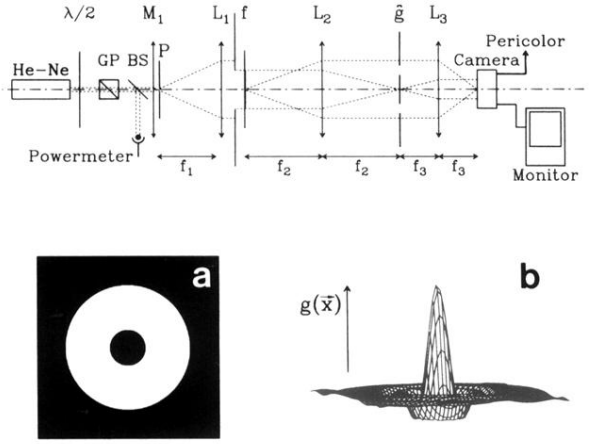

FIG. 1. Experimental setup. The intensity of the He-Ne laser is tuned by means of a half-wave plate associated with a Glan-prism (GP) polarizer, and monitored by means of a powermeter. *f*: fractal sample. (a) The Fourier transform $\hat{g}(\mathbf{q})$ of the analyzing wavelet; (b) the corresponding analyzing wavelet $g(\mathbf{x})$.

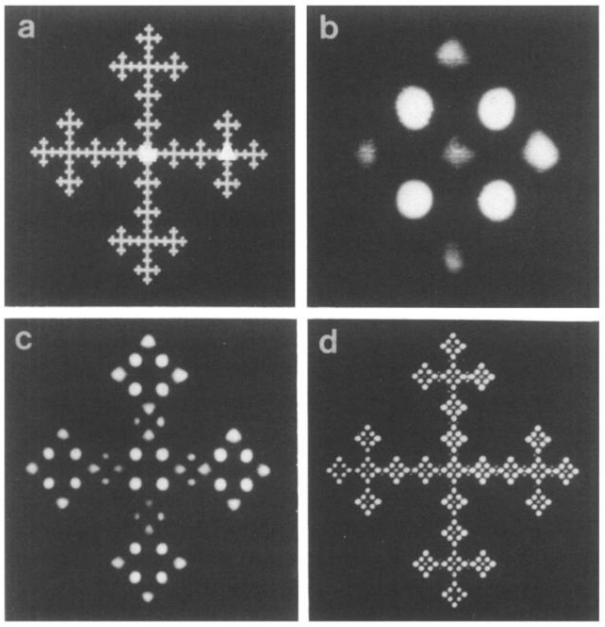

FIG. 2. (a) Snowflake fractal, and its OWT's at different scales: (b) $a = a^*/3$, (c) $a^*/3^2$, and (d) $a^*/3^3$. Pictures show rescaled intensities $S(a,\mathbf{b}) = a^{-\beta} I(a,\mathbf{b})$; $\beta = 2(\alpha_{SF} - 2)$, $\alpha_{SF} = \log 5/\log 3$.

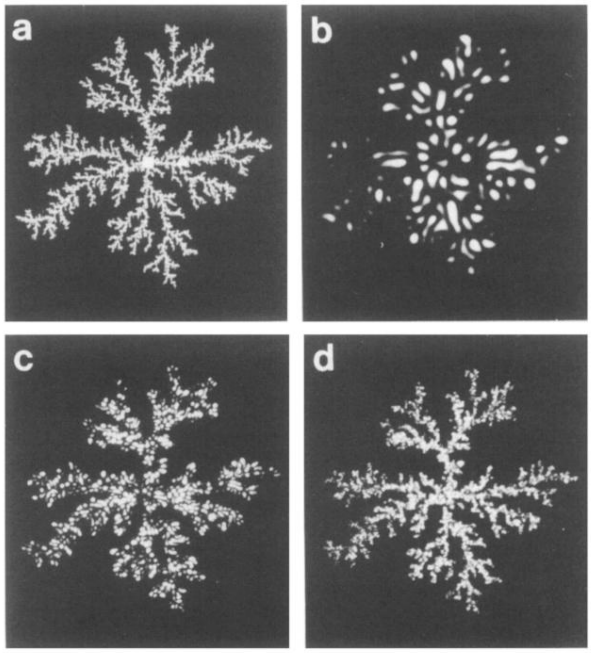

FIG. 3. (a) DLA fractal, and its OWT's at different scales: (b) $a = a^*$, (c) $a^*/3^{9/10}$, and (d) $a^*/3^{9/5}$. The intensity of the laser was tuned so as to keep the intensity maxima nearly independent of the filter size.